LETTER

doi:10.1038/nature16550

The temporal scaling of *Caenorhabditis elegans* ageing

Nicholas Stroustrup[1], Winston E. Anthony[1], Zachary M. Nash[1]†, Vivek Gowda[1], Adam Gomez[1]†, Isaac F. López-Moyado[1]†, Javier Apfeld[1]†§ & Walter Fontana[1]§

The process of ageing makes death increasingly likely, involving a random aspect that produces a wide distribution of lifespan even in homogeneous populations[1,2]. The study of this stochastic behaviour may link molecular mechanisms to the ageing process that determines lifespan. Here, by collecting high-precision mortality statistics from large populations, we observe that interventions as diverse as changes in diet, temperature, exposure to oxidative stress, and disruption of genes including the heat shock factor *hsf-1*, the hypoxia-inducible factor *hif-1*, and the insulin/IGF-1 pathway components *daf-2*, *age-1*, and *daf-16* all alter lifespan distributions by an apparent stretching or shrinking of time. To produce such temporal scaling, each intervention must alter to the same extent throughout adult life all physiological determinants of the risk of death. Organismic ageing in *Caenorhabditis elegans* therefore appears to involve aspects of physiology that respond in concert to a diverse set of interventions. In this way, temporal scaling identifies a novel state variable, $r(t)$, that governs the risk of death and whose average decay dynamics involves a single effective rate constant of ageing, k_r. Interventions that produce temporal scaling influence lifespan exclusively by altering k_r. Such interventions, when applied transiently even in early adulthood, temporarily alter k_r with an attendant transient increase or decrease in the rate of change in r and a permanent effect on remaining lifespan. The existence of an organismal ageing dynamics that is invariant across genetic and environmental contexts provides the basis for a new, quantitative framework for evaluating the manner and extent to which specific molecular processes contribute to the aspect of ageing that determines lifespan.

Body temperature is a major determinant of lifespan in poikilotherms[3–5] that also influences mammalian ageing[6]. From 20 °C to 33 °C, the mean lifespan of *C. elegans* decreases 40-fold[7]. To explore the impact of temperature on the actual distribution of lifespans, we used our automated imaging technology[8] to collect highly resolved mortality data in multiple replicate populations placed across this temperature range (Methods). From these data we estimated the survival curve $S(t)$, which is the probability of being alive at time (age) t, and the hazard function $h(t) = -\mathrm{d}\log S(t)/\mathrm{d}t$, which is the instantaneous risk of death at time t (Supplementary Note 1.1 and Methods).

In many invertebrates, changes in temperature alter the rate at which the risk of death increases with time[4,5,9]. Our lifespan data, controlled for environmental heterogeneity (see statistical methods section in Methods), confirmed this effect. However, we further observed that changes in temperature appeared to shift $h(t)$ by an equal and opposite amount in magnitude and time when plotted on a log–log scale, suggesting that between any two temperatures T_0 and T_1, $\lambda h_{T_1}(t) = h_{T_0}(\lambda^{-1}t)$ independent of any particular parametric form of $h(t)$. This change in hazard corresponds to a simple stretching of the survival function along the time axis by a dimensionless scale factor λ: $S_{T_1}(t) = S_{T_0}(\lambda^{-1}t)$ (Supplementary Note 1.2). The sole effect of changes in body temperature on lifespan therefore appeared to be a temporal rescaling of mortality statistics.

To confirm this effect, we applied an accelerated failure time (AFT) regression model[10] in which lifespan distributions that only differed by temporal scaling would have identically distributed residuals (Supplementary Notes 1.3 and 1.4 and Methods). To identify any significant differences between AFT residual distributions, we applied a Kolmogorov–Smirnov test adapted to censored data (Supplementary Note 2). We identified no significant temperature-dependent deviations from temporal scaling within two thermal ranges: 19–30 °C and 30.5–33 °C (Fig. 1b–d and Extended Data Figs 1–3). Populations above 30.5 °C exhibited a more pronounced late-age deceleration (Fig. 1e, Extended Data Fig. 3 and Supplementary Note 1.4), consistent with an increased heterogeneity[11] (Supplementary Note 3). Yet, even at high temperatures, the observed hazard function appears to be dominated more by ageing (for example, a progressive increase in the hazard) than by chance events that would produce a constant hazard (that is, non-ageing).

We then asked whether other interventions could produce a temporal scaling. Since oxidative damage has been linked to ageing across taxa[12,13], we quantified the effect of the oxidant *tert*-butyl hydroperoxide (tBuOOH) and found that it quantitatively rescales lifespan distributions in a dose-dependent manner up to 3 mM (Kolmogorov–Smirnov $P > 0.02$) with significant deviations observed only at 6 mM (Kolmogorov–Smirnov $P = 9 \times 10^{-4}$; Fig. 1f–g and Extended Data Fig. 4).

To further explore the range of interventions that might yield temporal scaling, we considered three members of the insulin/IGF-1 pathway[5,9]: *daf-16*, a transcription factor required for lifespan extension by multiple signals[14], *age-1*, a regulatory kinase upstream of *daf-16*, and *daf-2*, the insulin/IGF receptor, all of which influence both lifespan and thermal stress resistance[7]. Each mutant population exhibited a lifespan distribution rescaled from the wild-type distribution, both at 20 °C (Kolmogorov–Smirnov $P > 0.015$; Fig. 2a–e) and at 33 °C (Kolmogorov–Smirnov $P > 0.017$; Extended Data Fig. 4). The insulin/IGF receptor *daf-2* influences the activity of the heat shock factor *hsf-1* (ref. 15), and disruption of *hsf-1* also shortens lifespan by temporal rescaling (Kolmogorov–Smirnov $P > 0.2$; Fig. 2c, f). Elimination of the hypoxia-inducible transcription factor *hif-1*, known to influence lifespan through *daf-16*-dependent mechanisms[16], behaved likewise (Kolmogorov–Smirnov $P > 0.2$; Extended Data Fig. 4).

Since changes in nutrition alter lifespan across taxa[17], we considered two modifications of *C. elegans* diet: ultraviolet inactivation of the bacterial food source[18] and disruption of feeding behaviour by the *eat-2*(*ad1116*) mutation[19]. Ultraviolet inactivation of bacteria extended

[1]Department of Systems Biology, Harvard Medical School, Boston, Massachusetts 02115, USA. †Present addresses: Department of Microbiology and Immunology, School of Medicine, University of North Carolina at Chapel Hill, North Carolina 27599, USA (Z.M.N.); Department of Molecular, Cell, and Developmental Biology, University of California, Los Angeles, California 90095, USA (A.G.); Division of Signaling and Gene Expression, La Jolla Institute for Allergy and Immunology, La Jolla, California 92037, USA (I.F.L.-M.); Department of Biology, Northeastern University, Boston, Massachusetts 02115, USA (J.A.).

§These authors jointly supervised this work.

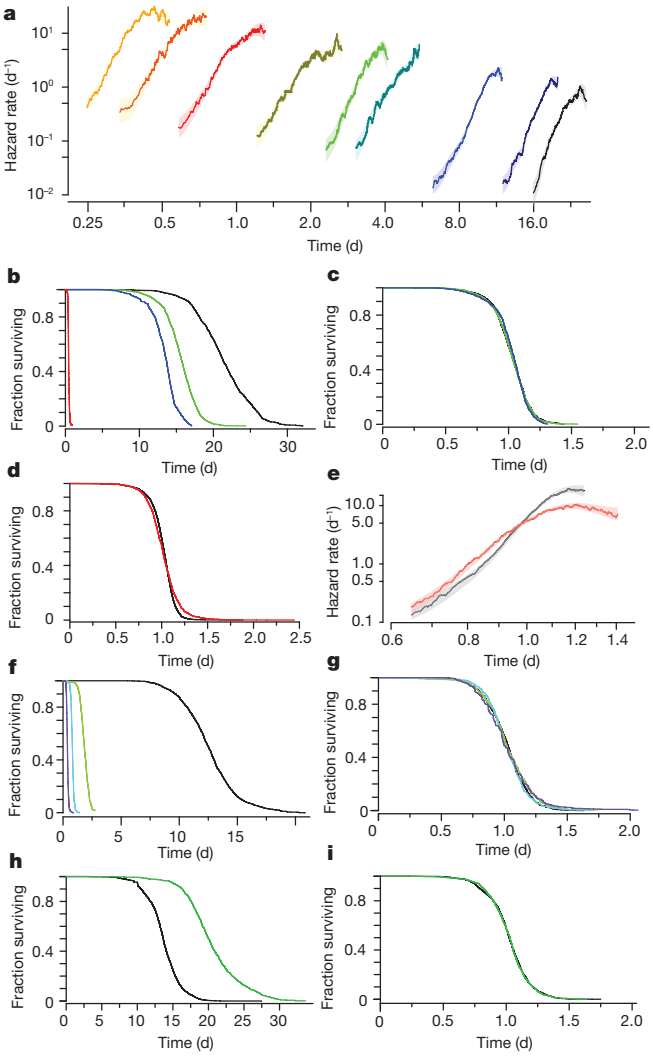

Figure 1 | Environmental determinants rescale *C. elegans* lifespan distributions. a, Populations grown at 20 °C were transferred on their second day of adulthood to a final temperature of (right to left) 20.1 °C (black), 23.7, 25.2, 29.1, 30, 30.9, 31.3, 32.5, and 32.6 (yellow). Individual lifespans were collected[7] and used to estimate the hazard function of each population using numerical differentiation of the Kaplan–Meier survival estimator (solid lines). The shaded areas represent the 95% confidence bands of the true hazard (Statistical methods). d, days. **b**, The lifespan of individuals living at 20, 25, 27, and 33 °C. **c**, The data in **b** were fitted with an AFT model $\log(y_i) = \beta x_i + \epsilon_i$ to remove differences in timescale (Methods and Supplementary Note 1.3). The AFT residuals $\exp(\epsilon_i)$ corresponding to populations at 20, 25, and 27 °C are plotted using the Kaplan–Meier survival estimator. **d**, The AFT residuals corresponding to populations held at 25 (black) and 33 °C (red) are plotted using the Kaplan–Meier survival estimator. **e**, Hazard functions were estimated from the 25 and 33 °C AFT residuals. **f**, The survival curves of populations exposed to 0 (black), 1.5 (blue), 3 (green), and 6 mM (purple) tBuOOH. **g**, The AFT residuals for the data of **f**. **h**, The survival curves of animals cultured on live *E. coli* (black) and ultraviolet-inactivated *E. coli* (green). **i**, The AFT residuals for the data of **h**.

lifespan via temporal scaling (Kolmogorov–Smirnov $P > 0.2$; Fig. 1h, i). In contrast, *eat-2*(*ad1116*) populations exhibited a significant deviation from temporal scaling (Kolmogorov–Smirnov $P = 5 \times 10^{-5}$), with a disproportionate increase in the standard deviation of lifespan compared with the mean (Fig. 2g, j). We also noted that *eat-2*(*ad1116*) populations exhibited a substantially increased variation in developmental timing. While such variation does not affect lifespan statistics based on manually synchronized young adults (Methods), it is possible that the causes of this developmental variation also underlie the increased variation of lifespan. We found that disruption of the mitochondrial complex I in *nuo-6*(*qm200*) populations produced analogous effects on developmental timing with a deviation from temporal scaling of lifespan similar to *eat-2*(*ad1116*) (Kolmogorov–Smirnov $P > 3 \times 10^{-18}$; Fig. 2h, k). Yet, populations with either allele exhibited temporally rescaled lifespan distributions in response to temperature changes (Kolmogorov–Smirnov $P > 0.2$; Fig. 2i, l and Extended Data Fig. 4). We conclude that while *eat-2*(*ad1116*), *nuo-6*(*qm200*), and shifts in temperatures from below to above 30 °C alter lifespan distributions outside the temporal scaling model, these interventions do not eliminate the ability of *C. elegans* to respond to subsequent interventions with temporal scaling. Temporal scaling thus appears to be a pervasive response to interventions of diverse modality and intensity.

Temporal scaling would arise if all physiological determinants of the risk of death in *C. elegans* acted as if they were jointly governed by a single stochastic process whose rate constant alone was altered by interventions (Supplementary Note 4). If the risk of death was determined in this way, we reasoned that transient interventions early in adulthood would produce a persistent temporal shift, not a scaling, of mortality statistics (Supplementary Note 4.3). To test this, we focused on temperature, which can be quantitatively, rapidly, and reversibly switched at any age between a baseline temperature T_0 and a transient temperature T_1 (Fig. 3a). We confirmed that transient exposure to higher temperatures produced a permanent shortening of lifespan[5] (Fig. 3b). We found that this shortening consisted of a temporal shift of the lifespan distribution (Fig. 3c, d) $S_{T_1}(t) = S_{T_0}(t - \Delta_\tau)$ that matches the magnitude of shift Δ_τ predicted if time were rescaled only for the period τ that animals were held at the transient temperature: $\Delta_\tau = \tau(1 - \lambda^{-1})$, with λ the scale factor relating populations always held at T_1 to populations always held at T_0 (Fig. 3e, f, Supplementary Note 4.3, Supplementary Table 2 and Extended Data Fig. 5). In a complementary experiment, we found that exposure to high temperature for different periods τ also gave shifts with the predicted magnitude (Extended Data Fig. 5). It appears, therefore, that the temporal scaling observed in Fig. 1a and the temporal shifting of Fig. 3 are compatible with a single model in which interventions alter the effective rate constant of a stochastic process governing those aspects of *C. elegans* physiology that determine risk of death. This process is evidently ongoing even very early in adulthood and is governed by the same rate constant as in late adulthood.

To clarify how molecular pathways contribute to temporal scaling, we quantified the magnitude of scaling produced by different intensities of intervention: that is, the scaling function. In the case of temperature, we applied an Arrhenius analysis[20,21] to interpret the change of λ (which in our framework rescales the rate constant of ageing) across the range 20–35 °C (Fig. 4a). We identified three distinct thermal regimes: I, 20–29.4 °C; II, 29.4–32.1 °C; III, 32.1–35 °C (Fig. 4b, Methods and Extended Data Figs 6 and 7) with regime I being further subdivided into Ia and Ib by a reproducible transition point at 24.4 °C.

Each scaling regime appears to correspond to a distinct molecular mechanism and barrier process dominating the timescale of ageing (Supplementary Table 1). Sharp decreases in lifespan have been observed to occur around 30 °C in *Drosophila melanogaster*[21], hinting at a more general phenomenon in poikilotherms. Notably, this transition coincided with a deviation from temporal scaling of lifespan distributions (Fig. 1e and Extended Data Fig. 3). Intriguingly, the scaling across the breakpoint between regimes Ia and Ib suggested that temporal scaling need not be disrupted by a change in the molecular mechanisms dominating the timescale of ageing.

Quantifying the effects of temperature on mutant strains, we found that the elimination of DAF-16 shorted lifespan by a rescaling of 28% in regime Ia and 25% in Ib (Fig. 4c, d). The *daf-16*(*mu86*) population exhibited the same slope in scaling function as wild type in Ia, and differed only by about 5% across regime Ib, suggesting that the mechanisms mediating the temperature dependence of lifespan

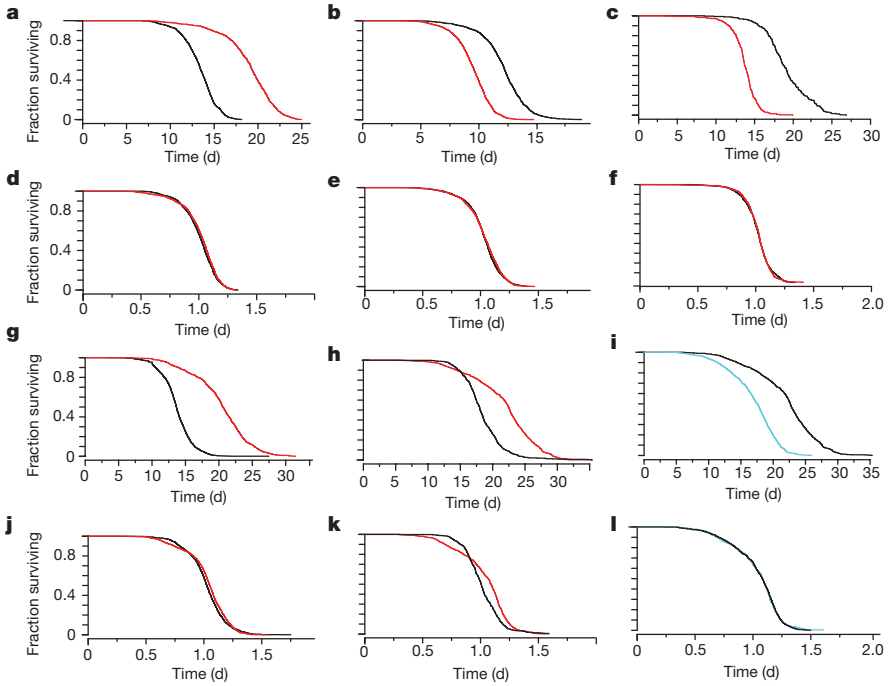

Figure 2 | Genetic determinants rescale *C. elegans* lifespan distributions. a–**c**, Survival curves are shown for *daf-2*(*e1368*) (red) and wild type (black) at 25 °C (**a**), *daf-16*(*mu86*) (red) and wild type (black) at 25 °C (**b**), and *hsf-1*(*sy441*) (red) and wild type (black) at 20 °C (**c**). **d**–**f**, The AFT residuals corresponding to the data in **a**–**c** respectively. Survival curves are shown for *eat-2*(*ad1116*) (red) and wild type (black) at 20 °C (**g**), *nuo-6*(*qm200*) (red) and wild type (black) at 25 °C (**h**), and *nuo-6*(*qm200*) populations held at 20 °C and 25 °C (**i**). **j**–**l**, The AFT residuals corresponding to the data in **g**–**i** respectively.

in regime I were not altered by elimination of DAF-16. In contrast, the hypomorphic alleles *daf-2*(*e1368*) and *age-1*(*hx546*) exhibit clear temperature-dependent effects across regime I (Fig. 4c, d). Both genes influence lifespan at 20 °C and 35 °C primarily by suppressing *daf-16* activity[22], which itself appears independent of temperature. Thus, *daf-2*(*e1368*) and *age-1*(*hx546*) alleles appear to be neomorphic in respect of the temperature dependence of their regulation of DAF-16.

We found that tBuOOH decreased lifespan at concentrations above 750 μM, with λ decreasing as a power law (Fig. 4e and Methods). This suggests an overall mass-action kinetics for the chain of events linking the direct targets of tBuOOH to the rescaling of the lifespan

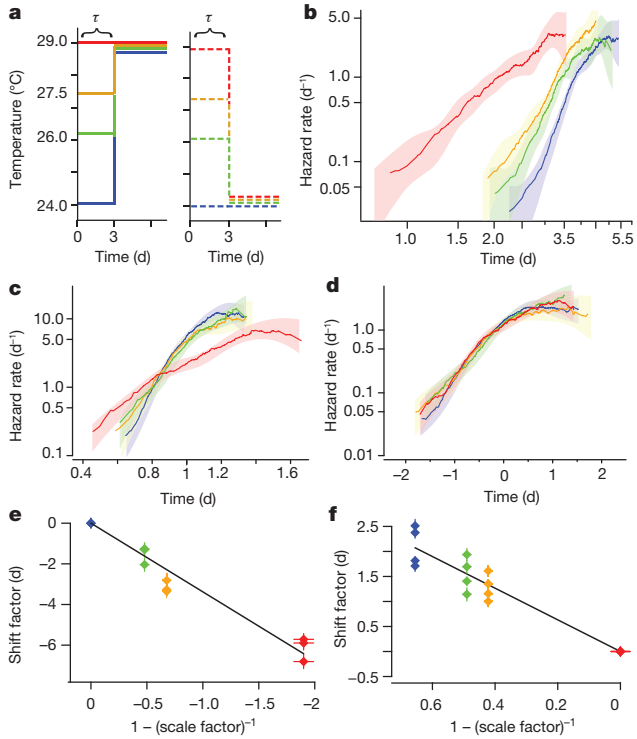

Figure 3 | Transient interventions during early adulthood shift the lifespan distribution. a, A schematic: populations were placed at 24 °C (blue), 26 °C (green), 27.5 °C (orange), and 29 °C (red). After $\tau = 3.2$ days, sub-populations were transferred to either 24 °C or 29 °C for the remainder of their lives. **b**, The hazard rate was estimated using the remaining lifespan of populations transferred to the final temperature of 29 °C. **c**, To test for temporal scaling between the populations shown in **b**, death times were fitted with the regression model $\log(y_i) = \beta x_i + \epsilon_i$, in which $\exp(\beta_i)$ is the best estimate for the scale factor λ. The residuals $\exp(\epsilon_i)$ are plotted as hazard functions in the colour scheme of **a**. **d**, To test for temporal shifts between the populations shown in **b**, death times were fitted with the regression model $y_i = \beta x_i + \epsilon_i$, in which β_i is the best estimate for the shift term Δ_τ. The residuals ϵ_i are plotted as hazard functions in the colour scheme of **a**. **e**, The shift term Δ_τ for populations transferred from each high temperature to 24 °C was plotted against $1 - \lambda^{-1}$, where λ is the scale factor relating populations always held at the corresponding high temperature to those always held at 24 °C. The prediction $\Delta_\tau = \tau(1 - \lambda^{-1})$ suggests that these points should fall along a line with a slope equal to τ in **a**. A linear regression on these points model estimates $\tau = 3.38 \pm 0.17$. **f**, As in **e**, but for populations transferred from lower initial temperatures to the final higher temperature of 29 °C, producing the estimate $\tau = 3.16 \pm 0.14$.

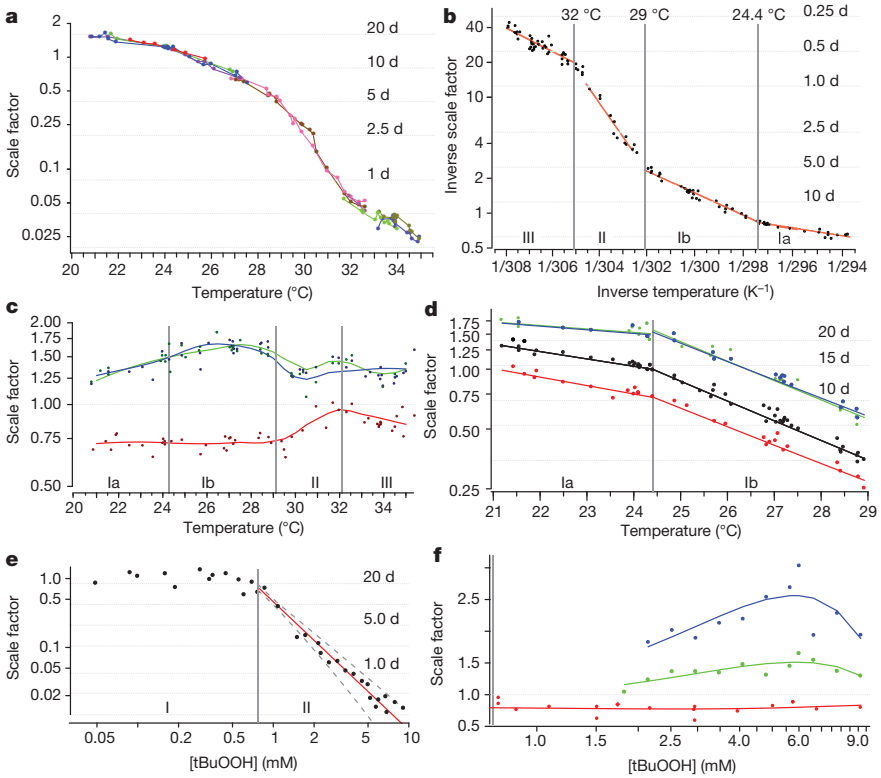

Figure 4 | Scaling functions. a, The magnitude of temporal scaling was estimated for wild-type populations held at fractional degree intervals across the range 20–35 °C. The scale factor λ of each population was estimated relative to a reference population at 25 °C. Grey lines mark the average lifespan of the reference population scaled by λ. Each replicate is shown as a separate colour, with each point corresponding to an aggregate population consisting of on average 130 individuals at the outset. **b**, The scale factor λ was determined for populations across the temperature range of **a**. The data points were fitted with a segmented Arrhenius model $\lambda(T)^{-1} = p_0 \exp(-p_1/RT)$ (red). **c**, The magnitude of scaling produced by *daf-16*(*mu86*) (red), *daf-2*(*e1368*) (green), and *age-1*(*hx546*) (blue) alleles relative to wild type was estimated at each temperature considered (points). Solid curves represent trends across temperature as fitted by a Loess regression. **d**, The combined magnitude of scaling produced by each allele and change of temperature was estimated relative to a single wild-type population 24 °C; colours as in **c**. Regimes II and III are shown in Extended Data Fig. 7. **e**, Wild-type populations at 20 °C were exposed to a series of tBuOOH concentrations ranging from 0 to 10 mM. For each population, λ was calculated relative to an unexposed population (0 mM). Data for concentrations above 0.75 mM were fitted by the model $\lambda([\text{tBuOOH}]) = p_2([\text{tBuOOH}])^{p_3}$ (red), yielding $p_2 = 0.47 \pm 0.02$ and $p_3 = -1.86 \pm 0.15$. **f**, As in **c**, but for the tBuOOH dosage series.

distribution. The distinct scaling functions of tBuOOH (power law) and temperature (multiple Arrhenius regimes) further suggest distinct molecular targets and mechanisms through which each type of intervention rescales the lifespan distribution.

As with temperature, the elimination of DAF-16 in the presence of tBuOOH reduced lifespan by a constant amount (Fig. 4f), 19.5 ± 8.8%, across all concentrations tested. Taken together with our temperature data in Fig. 4c, these results suggest that DAF-16 acts antagonistically but in parallel to the mechanisms through which tBuOOH and temperature shorten lifespan. DAF-16, tBuOOH, and temperature appear to affect ageing through their influence on risk determinants downstream of all three. For example, DAF-16 might attenuate or mitigate certain types of error or damage regardless of how the errors are created. The magnitude of temporal scaling produced both by *daf-2*(*e1368*) and by *age-1*(*hx546*) alleles varied across tBuOOH concentrations (Fig. 4g), which seems yet another aspect of a quantitative stress-dependent regulation of DAF-16 present in these strains but absent in wild type.

Disruption of *daf-2*, *daf-16*, *hif-1* or *hsf-1* produces distinct metabolic, cell-biological, and behavioural effects[15,23], as do changes in diet[24], temperature[25], and exposure to tBuOOH[26]. Yet, temporal scaling arises independently of the molecular targets specific to each intervention and requires that all risk determinants be affected to the same extent. This suggests that ageing in *C. elegans* can be described in terms of a whole-organism state variable r that completely determines all-cause mortality (Extended Data Fig. 9). State variables familiar from other contexts include temperature, pressure, and entropy, all of which describe the behaviour of a system resulting from the collective action of its many constituent elements without reference to their nature. In the same way, the change of the state over time, $r(t)$, describes the ageing process of *C. elegans* in terms of a collective action of all physiological determinants of risk. Where multiple risk determinants independently influence lifespan, temporal scaling requires that interventions simultaneously rescale, to an identical extent throughout life, the risk functions associated with each determinant (Supplementary Note 5.1). In models including dependencies among risk determinants, temporal scaling can emerge even when interventions act differentially across risk determinants (Supplementary Notes 5.2 and 5.3): dependencies can propagate the influence of interventions from one to all risk determinants, in effect producing a system-wide property that we call $r(t)$.

The temporal scaling of lifespan distributions constrains the dynamics of the state variable $r(t)$: the single stochastic process determining *C. elegans* lifespan must be invariant to timescale transformations and follow an average dynamics governed by an effective rate constant: $dr/dt = -k_r F(r)$, where $F(r)$ is an unknown function of r that does not depend on k_r. In this formulation, temporal scaling arises when interventions change k_r into k_r/λ. These dynamics place constraints on any stochastic process proposed to describe organismal ageing, as its parameters must change in a coordinated fashion. For example, if $r(t)$ were described by a biased random walk[27], the drift coefficient and the square of the diffusion coefficient must remain in a fixed proportion under intervention (Supplementary Note 6).

The idea that ageing is driven by changes in an organismal physiological state has been variously framed in terms of notions such as organization, vitality, organ reserve or resilience[3,28,29]. The temporal scaling across interventions justifies this notion, allowing an initial formalization. We note that any aspects of *C. elegans* physiology that change over time but do not influence lifespan, influencing 'quality' rather than 'quantity' of life, need not change in concert with $r(t)$.

We know neither the physiological basis of the state $r(t)$ nor the specific dynamics by which it changes with age. Yet, we can expect a broad set of lifespan determinants to affect only k_r, including minimally all determinants that influence lifespan exclusively through DAF-16 (refs 14 and 30), HSF-1 or HIF-1, or through the mechanisms that mediate the effects of temperature and tBuOOH on lifespan. If most ageing mechanisms currently studied influence only k_r, then future studies directed at clarifying the physiological origins of r and its dynamics should identify novel ageing mechanisms $F(r)$.

Online Content Methods, along with any additional Extended Data display items and Source Data, are available in the online version of the paper; references unique to these sections appear only in the online paper.

Received 27 July; accepted 18 December 2015.
Published online 27 January 2016.

1. Pincus, Z., Smith-Vikos, T. & Slack, F. J. MicroRNA predictors of longevity in *Caenorhabditis elegans*. *PLoS Genet.* **7,** e1002306 (2011).
2. Herndon, L. A. *et al.* Stochastic and genetic factors influence tissue-specific decline in ageing *C. elegans*. *Nature* **419,** 808–814 (2002).
3. Shaw, R. F. & Bercaw, B. L. Temperature and life-span in poikilothermous animals. *Nature* **196,** 454–457 (1962).
4. Mair, W., Goymer, P., Pletcher, S. D. & Partridge, L. Demography of dietary restriction and death in *Drosophila*. *Science* **301,** 1731–1733 (2003).
5. Wu, D., Rea, S. L., Cypser, J. R. & Johnson, T. E. Mortality shifts in *Caenorhabditis elegans*: remembrance of conditions past. *Aging Cell* **8,** 666–675 (2009).
6. Conti, B. *et al.* Transgenic mice with a reduced core body temperature have an increased life span. *Science* **314,** 825–828 (2006).
7. Lithgow, G. J., White, T. M., Melov, S. & Johnson, T. E. Thermotolerance and extended life-span conferred by single-gene mutations and induced by thermal stress. *Proc. Natl Acad. Sci. USA* **92,** 7540–7544 (1995).
8. Stroustrup, N. *et al.* The *Caenorhabditis elegans* lifespan machine. *Nature Methods* **10,** 665–670 (2013).
9. Johnson, T. E., Wu, D., Tedesco, P., Dames, S. & Vaupel, J. W. Age-specific demographic profiles of longevity mutants in *Caenorhabditis elegans* show segmental effects. *J. Gerontol. A* **56,** B331–B339 (2001).
10. Swindell, W. R. Accelerated failure time models provide a useful statistical framework for aging research. *Exp. Gerontol.* **44,** 190–200 (2009).
11. Vaupel, J. W., Manton, K. G. & Stallard, E. The impact of heterogeneity in individual frailty on the dynamics of mortality. *Demography* **16,** 439–454 (1979).
12. Martin, G. M., Austad, S. N. & Johnson, T. E. Genetic analysis of ageing: role of oxidative damage and environmental stresses. *Nature Genet.* **13,** 25–34 (1996).
13. Tullet, J. M. *et al.* Direct inhibition of the longevity-promoting factor SKN-1 by insulin-like signaling in *C. elegans*. *Cell* **132,** 1025–1038 (2008).
14. Landis, J. N. & Murphy, C. T. Integration of diverse inputs in the regulation of *Caenorhabditis elegans* DAF-16/FOXO. *Dev. Dyn.* **239,** 1405–1412 (2010).
15. Hsu, A. L., Murphy, C. T. & Kenyon, C. Regulation of aging and age-related disease by DAF-16 and heat-shock factor. *Science* **300,** 1142–1145 (2003).
16. Leiser, S. F., Begun, A. & Kaeberlein, M. HIF-1 modulates longevity and healthspan in a temperature-dependent manner. *Aging Cell* **10,** 318–326 (2011).
17. Kirkwood, T. B. & Shanley, D. P. Food restriction, evolution and ageing. *Mech. Ageing Dev.* **126,** 1011–1016 (2005).
18. Garigan, D. *et al.* Genetic analysis of tissue aging in *Caenorhabditis elegans*: a role for heat-shock factor and bacterial proliferation. *Genetics* **161,** 1101–1112 (2002).
19. Lakowski, B. & Hekimi, S. The genetics of caloric restriction in *Caenorhabditis elegans*. *Proc. Natl Acad. Sc. USA* **95,** 13091–13096 (1998).
20. Suda, H., Sato, K. & Yanase, S. Timing mechanism and effective activation energy concerned with aging and lifespan in the long-lived and thermosensory mutants of *Caenorhabditis elegans*. *Mech. Ageing Dev.* **133,** 600–610 (2012).
21. Atlan, H., Miquel, J., Helmle, L. C. & Dolkas, C. B. Thermodynamics of aging in *Drosophila melanogaster*. *Mech. Ageing Dev.* **5,** 371–387 (1976).
22. Libina, N., Berman, J. R. & Kenyon, C. Tissue-specific activities of *C. elegans* DAF-16 in the regulation of lifespan. *Cell* **115,** 489–502 (2003).
23. Murphy, C. T. *et al.* Genes that act downstream of DAF-16 to influence the lifespan of *Caenorhabditis elegans*. *Nature* **424,** 277–283 (2003).
24. Walker, G., Houthoofd, K., Vanfleteren, J. R. & Gems, D. Dietary restriction in *C. elegans*: from rate-of-living effects to nutrient sensing pathways. *Mech. Ageing Dev.* **126,** 929–937 (2005).
25. McColl, G. *et al.* Insulin-like signaling determines survival during stress via posttranscriptional mechanisms in *C. elegans*. *Cell Metab.* **12,** 260–272 (2010).
26. Oliveira, R. P. *et al.* Condition-adapted stress and longevity gene regulation by *Caenorhabditis elegans* SKN-1/Nrf. *Aging Cell* **8,** 524–541 (2009).
27. Aalen, O. O. & Gjessing, H. K. Understanding the shape of the hazard rate: a process point of view. *Stat. Sci.* **16,** 1–14 (2001).
28. Medawar, P. B. *An Unsolved Problem of Biology: An Inaugural Lecture Delivered at University College, London* (H. K. Lewis, 1951).
29. Gladyshev, V. N. The origin of aging: imperfectness-driven non-random damage defines the aging process and control of lifespan. *Trends Genet.* **29,** 506–512 (2013).
30. Samuelson, A. V., Carr, C. E. & Ruvkun, G. Gene activities that mediate increased life span of *C. elegans* insulin-like signaling mutants. *Genes Dev.* **21,** 2976–2994 (2007).

Supplementary Information is available in the online version of the paper.

Acknowledgements We thank J. Alcedo for nematode strains, X. Manière for providing the NEC937 *Escherichia coli* strain, B. Ward for reading our manuscript, and D. Marks, C. Romero, T. Kolokotrones, D. Yamins, P. F. Stadler, E. Smith, and all members of the Fontana laboratory for discussions and encouragement throughout this project. Some strains were provided by the Caenorhabditis Genetics Center, which is funded by US National Institutes of Health (NIH) Office of Research Infrastructure Programs (P40 OD010440). This work was funded by the NIH through grant R01 AG034994 and by a Glenn Award from the Glenn Foundation for Medical Research.

Author Contributions N.S. conceived and analysed the experiments. N.S., J.A., W.E.A., V.G., A.G., Z.M.N., and I.F.L.-M. developed experimental protocols and performed experiments. N.S. and W.F. interpreted data and performed model calculations. N.S. and W.F. wrote the manuscript with input from J.A.

Author Information Reprints and permissions information is available at www.nature.com/reprints. The authors declare no competing financial interests. Readers are welcome to comment on the online version of the paper. Correspondence and requests for materials should be addressed to N.S. (nstroustrup@post.harvard.edu) or W.F. (walter@hms.harvard.edu).